

■ Computational chemistry

Unravelling Chemical Interactions with Principal Interacting Orbital Analysis

Jing-Xuan Zhang, Fu Kit Sheong,* and Zhenyang Lin*[a]

Abstract: Decomposing chemical interactions into bonds and other higher order interactions is a common practice to analyse chemical structures, and gave birth to many chemical concepts, despite the fact that the decomposition itself might be subjective in nature. Fragment molecular orbitals (FMOs) offer a more rigorous alternative to such intuition, but might be less interpretable due to extensive delocalisation in FMOs. Inspired by the Principal Component Analysis in statistics, we hereby present a novel framework, Principal Interacting Orbital (PIO) analysis, that can very quickly identi-

fy the “dominant interacting orbitals” that are semi-localised and easily interpretable, while still maintaining mathematical rigor. Many chemical concepts that are often taken for granted, but could not be easily inferred from other computational techniques like FMO analysis, can now be visualised as PIOs. We have also illustrated, through various examples covering both organic and inorganic chemistry, how PIO analysis could help us pinpoint subtle features that might play determining roles in bonding and reactions.

Introduction

Understanding how two chemical fragments interact with each other, based on their electronic structures, is a fundamental exercise in chemistry. Such fragment-based analysis is the central pillar of numerous chemical concepts, influencing chemistry in different aspects, ranging from the investigation of chemical structures to the tuning of functional groups for promoting reactions.^[1–7] In both organic and inorganic chemistry, classifying the chemical interactions involved in a structure or a reaction is always an indispensable part of our understanding of chemistry.


Traditionally, chemical interactions are often elucidated by a divide-and-conquer approach. One first divides a molecule into two or more moieties, and then considers the interactions between, or among, the moieties in a localised (often pairwise) manner. These interactions are often taken into account in the order of their relative importance, that is, “bonds” are considered before higher order effects like conjugations or back-donations. This hierarchical approach dominates the chemists’ philosophy, not just because of its intuitiveness, but also its century-old success in giving insights into experimental observations and even predictions.

With the development of quantum chemical theories and related computational techniques, another more sophisticated approach of understanding chemical interactions has emerged: the orbital interaction approach. Pioneered by Kenichi Fukui and Roald Hoffmann, orbital interaction is a framework founded on quantum mechanics that allows a bird’s-eye view of chemical phenomena.^[1–4,6,7] From the simplest head-on orbital overlap between two methyl groups giving rise to a covalent bond, to the more complicated mutual delocalisation driving a Diels–Alder (DA) reaction (both examples will be discussed in detail in this work), chemists have conveniently explained the nature of many experimentally observed phenomena through the orbital interaction approach.

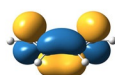
When applying the orbital interaction approach to describe the interaction of two fragments, the “canonical molecular orbitals” (eigen-orbitals of a Fock operator in the HF/DFT method to be precise,^[8] often simply referred to as molecular orbitals, or MOs, which will be adopted in this work when no ambiguity arises) of each fragment are often used. For the simplest Diels–Alder reaction, orbital interaction is pictured as the HOMO and LUMO of butadiene interacting with the LUMO and HOMO of ethene, respectively. Because MOs are adapted to molecular symmetry, one can invoke the symmetry argument when analysing the orbital interactions in a reaction. For example, the cycloaddition reaction between two ethene molecules in a concerted [2+2] manner is symmetry-forbidden, and is thus unlikely to occur under thermal conditions.^[1] An apparent advantage of using fragment MOs (FMOs) is its transferability across different reaction counterparts, which gives rise to a wide use of HOMO/LUMO for analysing nucleophilicity/electrophilicity.

Despite the apparent success of using fragment MOs for analysing orbital interactions, one can often find cases in which

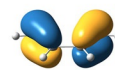
[a] J.-X. Zhang, Dr. F. K. Sheong, Prof. Z. Lin
Department of Chemistry
The Hong Kong University of Science and Technology
Clear Water Bay
Kowloon, Hong Kong (P.R. China)
E-mail: fksheong@connect.ust.hk
chzlin@ust.hk

 Supporting information and the ORCID identification number(s) for the author(s) of this article can be found under:
<https://doi.org/10.1002/chem.201801220>

(a) MOs of butadiene

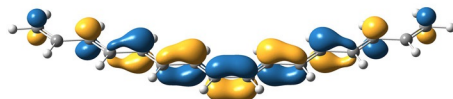


LUMO

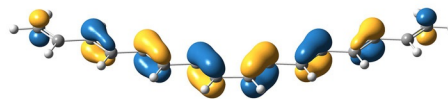


HOMO

(b) MOs of hexadecoctaene



LUMO



HOMO

(c) PIOs of hexadecoctaene upon reaction with ethene

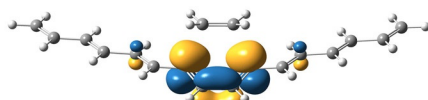
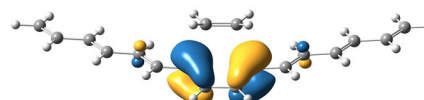
1st PIO2nd PIO

Figure 1. Comparisons of PIOs and MOs in a hypothetical DA reaction. (a) MOs of hexadeca-1,3,5,7,9,11,13,15-octaene. (b) MOs of buta-1,3-diene. (c) PIOs of hexadeca-1,3,5,7,9,11,13,15-octaene with respect to ethene in the transition state of their Diels–Alder reaction. Note that PIOs are semi-localised and more resemble MOs of the sub-system, or in the other words, the interacting orbitals which are consistent with chemical intuition. Isovalue: 0.05.

the involved atoms hinted by fragment MOs are not necessarily those suggested by conventional wisdom. To better illustrate this point, let us consider the Diels–Alder-type [4+2] reaction between a long-chain polyene and ethene. It is natural to assume only two adjacent double bonds in polyene are involved in the reaction, and the remaining double bonds are not significantly involved. One might therefore expect the “interacting orbitals” to be localised on the adjacent double bonds under consideration closely resembling those of butadiene (Figure 1(a)). However, when we analyse the frontier MOs of the polyene, the HOMO and LUMO are both spread out over the whole molecule (Figure 1(b)).

One may be tempted to conclude that our “intuitive picture”, despite its usefulness in practical application, has no theoretical foundation, judging from the obvious inconsistency between intuition and computed fragment MOs. But this inconsistency actually arises from the fact that we chose “canonical” fragment MOs for studying orbital interactions. We will show in this work that there exists a unitary transformation within the set of the occupied “canonical” molecular orbitals, giving an equivalent total wavefunction and providing linear combinations of the molecular orbitals that well-resemble the “localised MOs”, and are consistent with chemists’ intuition. A great advantage of localised MOs is substituent invariance, as substituents are often observed to have only perturbative effects on the main reaction site. Such invariance serves as the basis of the “functional group” concept, one of the most important concepts in chemistry.

To allow a seamless connection between quantum chemical calculations and chemical intuitions, many efforts have been devoted to seek for a set of localised orbitals (through a transformation of MOs) that best represents chemists’ intuition on both electronic structures and orbital interactions in molecules.^[8,9] A widely recognised attempt should be attributed to Wienhold and his co-workers,^[10–12] who utilised the properties

of a density matrix to construct Natural Atomic Orbitals (NAOs) and Natural Bond Orbitals (NBOs). NBOs form a localised representation of bonding in molecules that is usually in a good correspondence with the classic Lewis structure description. As a result, NBOs have earned a reputation of being known as “the chemists’ basis set”.^[11] In spite of these advantages, if we apply the NBO method to understand the Diels–Alder reaction between a long-chain polyene and ethene, the NBO method would only identify a number of localised double bonds in the polyene (see below); a picture that is still inconsistent with the butadiene-like “localised” HOMO/LUMO. In the literature, there are also several other approaches aimed at dealing with complicated systems with non-classical interactions.^[12–17] For example, Charge Decomposition Analysis (CDA) is very useful for quantitative description of donor-acceptor interactions.^[13] Another recently developed method, Adaptive Natural Density Partitioning (AdNDP), extends the idea of NBO by searching multi-centred bonds beyond 2- or 3-centred bonds,^[14] which provides better applicability than NBO on certain cluster compounds.^[18–20] Still, a unified analysis framework that could be generically applied to a wide range of chemical compounds is lacking.

In this work, we are going to present a novel approach to study chemical interactions, which takes advantage of both the rigor of quantum chemical interaction and the intuitiveness of a localised (or semi-localised) picture, without sacrificing its general applicability to a wide range of chemical systems. The key idea is to take into account fragmentation during the analysis, and find the recombination of the orbitals within a fragment that interacts the most with the other fragment. By applying two rounds of Principal Component Analysis^[21] (PCA) (a simple yet powerful mathematical tool in statistics) to the off-diagonal block of the NAO-based density matrix (Figure 2), we can not only easily identify all such orbitals, which we would like to name “Principal Interacting Orbitals”

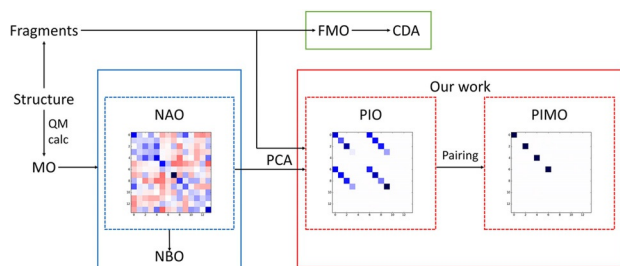


Figure 2. A flow chart demonstrating how PIOs are obtained. The matrices shown here are only for demonstration purpose. Note that the density matrix is block-wise diagonalised in the PIO representation and fully diagonalised in the PIMO representation under certain conditions (see Methods for details).

(PIOs), but also quantify their contributions to the overall fragment interaction. We found that the quantified contributions could be easily interpreted in a way that mirrors the hierarchical view in chemists' intuition, in the sense that the top PIOs are those dominantly involved in chemical bonding, and the succeeding PIOs reflect various secondary interactions (if present), as demonstrated by the presented examples. We have also proven that the PIOs can be combined in a pairwise manner to obtain "Principal Interacting Molecular Orbitals" (PIMOs), representing the bonding and anti-bonding orbitals that arise from orbital interactions. A wide range of examples covering both inorganic and organic chemistry has been presented, to demonstrate how PIO analysis could be applied to analyse chemical structures as well as reactions. We anticipate this approach could be applied to more complicated systems to unravel chemical interactions and help us gain in-depth chemical insights.

Results and Discussion

We would like to begin with a brief summary of the PIO work flow as follows:

1. One first carries out normal quantum chemistry calculations, followed by natural population analysis to obtain the NAO coefficients and NAO-based density matrix.
2. The PIO program reads in a fragmentation scheme (two groups of atom IDs) to partition the density matrix into blocks.
3. Two rounds of PCA are performed to rearrange the orbitals of each fragment (see Methods for algorithmic details). After this step, the off-diagonal block will be diagonalised (Figure 2), implying a 1-to-1 interacting pattern, hence the PIOs of two fragments naturally form pairs. The element in the PIO-based off-diagonal block corresponding to a PIO pair, which describes the magnitude of interaction between the associated PIO pair, is named the PIO-based Bond Index (PBI). The diagonal elements of the PIO-based density matrix represent the populations of PIOs. The orbital energy associated with each PIO can be obtained by performing the same transformation on the Fock matrix if needed.

4. For HF/DFT calculations with full fragmentations, the whole density matrix will be block-wise diagonalised in step 3 (see Methods for a proof of this). Hence a further diagonalisation of the whole density matrix can be realised by pairing up each PIO pair, and the resulting orbitals are named PIMOs (which form a particular choice of natural orbitals).

To illustrate how the PIO method helps us analyse electronic structures of chemical systems, we have selected several different examples covering both organic and inorganic chemistry, as discussed in the following subsections. We will also show how such analysis could impact our study and understanding of chemical structures and reactions.

Classic examples

Analysing a molecule from a chemist's point of view usually involves decomposing the interaction between fragments into primary interactions (usually covalent bonds), secondary interactions (hydrogen bonds, conjugations, electron donating and withdrawing effects of substituents, back-donations in coordination complexes, etc.) and high-order interactions. Such a hierarchical understanding of chemistry enables us to extract the most important information from a huge amount of data.

This mindset could be well illustrated using one of the simplest molecules, ethane. Ethane contains two equivalent methyl groups connected by a single bond, while the hyper-conjugation effect has been considered as a factor leading to the favourable staggered conformation of ethane.^[22,23] Such decomposition of interactions between two methyl groups into σ -bond and hyper-conjugation follows the aforementioned hierarchical understanding of chemistry.

In this regard, our PIO analysis could be applied to identify and quantify these interactions. We partition the ethane molecule into two methyl groups and carry out our PIO analysis, and the results are shown in Figure 3. We can clearly see that the first PIO of each fragment is an sp -hybridised orbital of the carbon atom, and the pair from both fragments forms a σ -bond that dominates the interactions between the two methyl groups (over 90% contribution to the total). Readers familiar with NBO analysis might find the first pair of PIOs similar to two Natural Hybrid Orbitals, but subsequent PIO pairs reveal that they are fundamentally different, in the sense that multi-atom contribution is allowed in a PIO (which will be better illustrated in the following examples). A pair of localised MOs (PIMOs) arises from the orbital interaction of a PIO pair, which is obtained by proper in-phase and out-of-phase combinations of the corresponding PIO pair. The resulting PIMO pair can be understood as the local bonding and anti-bonding orbitals as one may encounter in the textbook schematics (Figure 3(c)).

The hyper-conjugations between the two methyl groups are less dominant and are represented by the 2nd to 5th PIO pairs, each reflecting some electron delocalisation from the C–H bonds of one methyl group to the C–H anti-bonding orbitals of the other methyl group. Note that we have four such interactions that are all degenerate because of the symmetric fragmentation, as well as the intrinsic D_{3d} symmetry of ethane. The

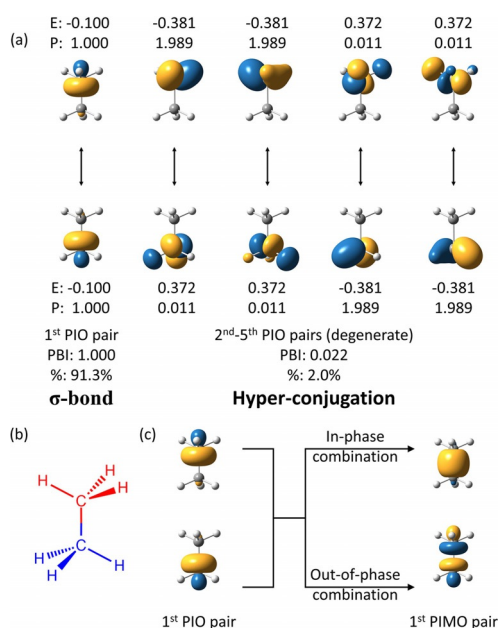


Figure 3. Results of PIO analysis on ethane with two methyl groups as two fragments. (a) The top five PIOs of each fragment. The orbital energies and populations (occupation numbers) are given as E and P, respectively, near each PIO. Given below each PIO pair are the PIO-based bond indices (abbreviated as PBI) and its contribution (as %) to the total interactions between two fragments (the contributions of all PIOs sum up to 100%). (b) The Scheme of fragmentation of ethane into two methyl groups (fragments) carried out in the PIO analysis. (c) The first PIMO pair and its relationship with the first PIO pair. Note that the phase of each PIO is naturally paired up with its counterpart from our algorithm (see Methods for detail). Isovalue: 0.10 for all orbitals.

next few PIO pairs are even weaker hyper-conjugations or other high-order interactions. Interested readers can refer to the Supporting Information for the visualisation of these orbitals.

A better example to illustrate hyper-conjugation might be the *tert*-butyl cation. It is well-known that the carbocation is stabilised by the hyper-conjugation with surrounding C–H bonds.^[24,25] This fact can be easily captured by PIO analysis by cutting the molecule into a methyl group and a dimethylmethylene (see Figure 4). The first PIO pair apparently represents the σ -bond between the two fragments, having a PBI very close to one. The hyper-conjugation effect can be clearly seen from the next PIO pair which consists of an almost pure p-orbital of the central carbon of dimethylmethylene, and a combination of multiple C–H bonds in methyl. The associated PBI is 0.279, indicating that the electron delocalisation due to hyper-conjugation is much more prominent here than that in ethane.

A slightly more sophisticated example is $[\text{Re}_2\text{Cl}_8]^{2-}$, which is a very famous example containing a metal-metal δ -bond.^[30,31] Again the metal-metal bonding picture can be described by PIOs in a very straightforward manner; namely the top four PIOs of a ReCl_4 fragment are one σ -, two π - and one δ -type metal d-orbitals, each interacting with an identical d-orbital of the other ReCl_4 fragment with a PBI of exactly one (see Figure 5). Contributions from orbitals of chlorides can hardly

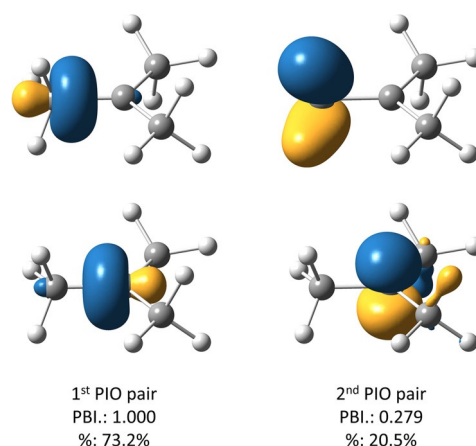


Figure 4. Results of PIO analysis on *tert*-butyl cation with a methyl group as one fragment and dimethylmethylene as the other. Isovalue: 0.10.

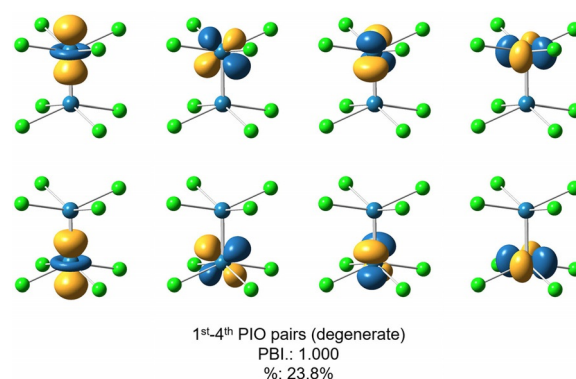


Figure 5. Results of PIO analysis on $[\text{Re}_2\text{Cl}_8]^{2-}$, each $[\text{ReCl}_4]$ moiety being one fragment. Isovalue: 0.10.

be seen in the top four PIO pairs. On the other hand, some dp-hybridisation can be observed in the 2nd and 3rd PIO pairs, due to the distorted square-planar geometry of each metal centre.

From these very simple examples we can see that the dominant bonding interactions can be easily captured by PIO analysis, and the chemical interaction hierarchy can also be well illustrated. We have demonstrated the power of using PIO analysis to reinstate many empirical chemical concepts in a quantitative manner. Hierarchical understanding is naturally achieved by examining one-by-one all the PIOs, sorted in a decreasing order of contribution. More examples of such hierarchical decomposition could be found in Supplementary Information Figures S3 to S20, including, but not limited to, the aforementioned primary and secondary orbital interactions. These serve as a demonstration of how PIO analysis helps us link the results of quantum chemical calculations to the large collection of chemical concepts we have. In this sense, one of the most important advantages of our PIO analysis is its capability to systematically identify and quantify orbital interactions with vastly different magnitudes, which is seldom achievable with other current computational tools.

Diels–Alder reactions

One of the most famous early applications of fragment orbital interaction might be the Diels–Alder (DA) reaction.^[1] It has been proposed by the Nobel laureate Kenichi Fukui that the DA reaction should be described as a mutual delocalisation between the diene and dienophile substrates.^[4] To be specific, the HOMO of the diene interacts with the LUMO of the dienophile in the reaction, whereas the LUMO of the diene interacts with the HOMO of the dienophile at the same time (Figure 6(a)). Such a concept has been widely used to understand the regio-selectivity of DA reactions.^[1,24]

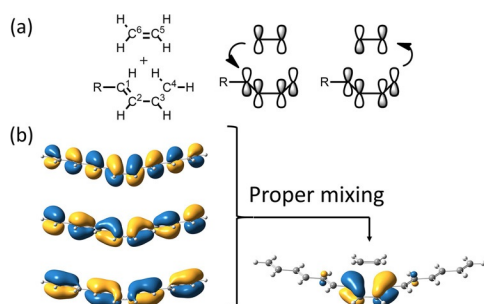


Figure 6. Orbital interactions in a DA reaction. (a) A schematic plot of orbital interactions that dominate the reaction. (b) A schematic plot showing the relationship between FMOs and PIOs.

However, one should note that in this picture, we have ignored the existence of the R group and its effect on MOs. By doing so, we implicitly separate the “substituent” from “reactive functional group”, to allow an orbital picture that is substituent-invariant. For a similar reason, the “HOMO/LUMO” that has been used to describe the DA reaction should not be taken as the real HOMO/LUMO of the two substrates, but is more like a “local HOMO/LUMO” at the reaction site that resembles the HOMO/LUMO of simple butadiene and ethene. An extreme but apparent example is the DA reaction between a hexadeca-1,3,5,7,9,11,13,15-octaene and an ethene. The HOMO and LUMO of hexadeca-octaene are apparently delocalised over the whole molecule (Figure 1(b)), whereas chemists would instead prefer to describe the hexadeca-octaene simply as a substituted butadiene, and then use the butadiene model to understand the reaction, even though the theoretical foundation of such practice might not be obvious.

On the other hand, when we perform the PIO analysis on this hypothetical DA reaction, the dominant PIOs of the polyene with respect to dienophile indeed resemble the HOMO/LUMO of an unsubstituted butadiene (Figure 1(c)). One can see that these PIOs are mainly localised on the “reactive functional group” and have only a minor effect from the substituents, consistent with our substituent-invariant understanding. This ability to localise orbitals to the reactive part (compared to FMOs), while preserving the necessary multi-centred feature is one main advantage of PIO analysis over traditional FMO analysis.

To understand the relationship between FMO and PIO, one can consider each PIO as a linear combination of FMOs, such that the resulting orbital has the strongest interaction with the other fragment (Figure 6(b)). Such a definition does not mandate PIOs to be localised, although the maximisation of interaction usually makes it the case. As a result, PIO analysis achieves a balance between localisation of orbitals and the delocalised nature of electrons, especially when the interaction involves multiple sites.

There are also other methods that aim at obtaining localised descriptions of electronic structures, including the well-known NBO method and the recently developed AdNDP method. However, the way that orbitals are localised is usually determined by predefined (either built-in or specified by users) parameters in these methods. The need of such hard thresholds may lead to ambiguity in describing chemical structures or unphysical discontinuity when tracing reactions. To fully illustrate this point, we take the simplest DA reaction between butadiene and ethene as an example.

Shown in Figure 7 are the results obtained from three different methods, namely PIO, NBO and AdNDP. When applied to analyse the transition state of this reaction, we can immediately see that these methods have completely different results. While the PIO analysis provides two pairs of orbital interactions that correspond well with our understanding of a DA reaction, the NBO method gives three localised double bonds instead.

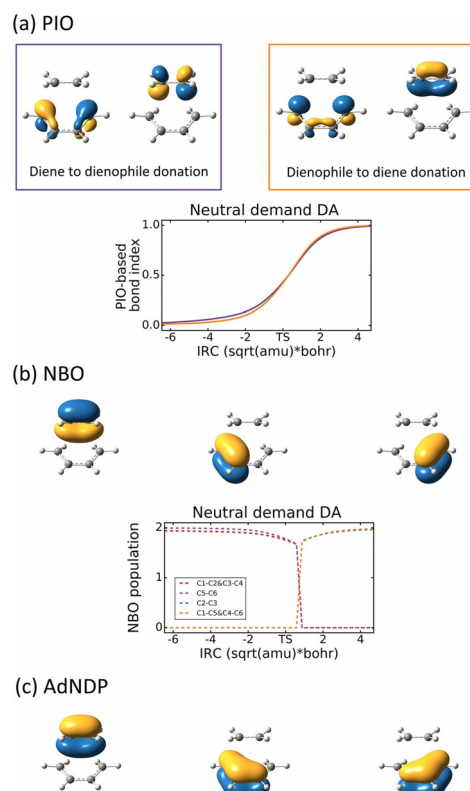


Figure 7. Comparison of PIO with NBO and AdNDP methods. (a) The top two PIOs of the interacting fragments in the TS of DA reaction, and the trace of PBI along IRC. (b) Three selected NBOs in the TS of DA reaction and the trace of NBO populations along IRC. (c) Three selected multi-centred orbitals calculated by AdNDP.

Moreover, when we carry out the intrinsic reaction coordinate (IRC) calculation and perform NBO analysis on each point, the results do not change continuously. At a certain stage, the results would suddenly switch from three π -bonds to three newly formed bonds, which is unphysical. On the other hand, PIO analysis gives a constantly varying result when the reaction proceeds. This kind of difference comes from the fact that the NBO method is highly parameterised, whereas PIO analysis is completely parameter-free. A parameter-dependent method would easily encounter boundary cases when the system continuously varies.

In terms of continuous tracing over a reaction, AdNDP pushes such an anomaly to the limit, because users' parameter input is required by design.^[14] However, there is not any systematic approach to determine which set of parameters should be used. In this example, one set of parameters would lead to exactly the same results as the NBO method, whereas another set of parameters would result in the orbitals as shown in Figure 7(c). For this reason, we did not trace the AdNDP results along IRC. In addition, the AdNDP algorithm has to search over an exponentially increasing number of possible combinations of atoms when determining a multi-centred bond, which is unaffordable for large systems,^[14] whereas PIO analysis only involves a constant number of matrix diagonalisation steps, and is usually completed in seconds for calculations with about one thousand basis functions in an ordinary personal computer.

Tracing PBI over the reaction coordinate can also reveal other properties of the reaction. For example, it is known that there exist three different types of electron demand in DA reactions, according to the relative strength of the two aforementioned orbital interactions.^[24] When there are electron-donating groups (EDGs) on the diene and electron-withdrawing groups (EWGs) on the dienophile, the interaction between the HOMO of the diene and LUMO of the dienophile is stronger, and this scenario is called a normal demand DA reaction. The opposite scenario, where there are EDGs on the dienophile

and EWGs on the diene, and the interaction between the LUMO of the diene and the HOMO of the dienophile becomes more significant, is termed an inverse demand DA reaction. When two interactions are comparable, the reaction is named a neutral demand DA reaction. As we can obtain the contribution of each PIO pair to overall interactions, we should be able to distinguish DA reactions with different electron demands through PIO analysis. This point can be elucidated by performing PIO analyses on every point along the IRC calculation of each system and the results are summarised in Figure 8.

From the results of PIO analysis on the selected systems, the first observation is that the interactions between diene and dienophile are indeed dominated by the two pairs of orbitals that resemble the HOMO/LUMO of butadiene and ethene, respectively. The cumulative contribution of the top two PIO pairs is over 90% in the transition states and products, and is over 80% throughout the available IRC range for every system. At the end of all reactions, the top two PIO pairs have a PBI of nearly one, representing the two newly formed σ -bonds in the final products.

Moreover, we can clearly see a preference of orbital interaction in each of the three systems as expected. The purple PIO pair (HOMO of diene and LUMO of dienophile) has a stronger interaction in the normal demand DA reaction, whereas the orange pair (LUMO of diene and HOMO of dienophile) dominates in the inverse demand DA reaction. In the neutral demand DA reaction between butadiene and ethene, the purple pair and orange pair contribute almost equally, which is most consistent with Fukui's mutual delocalisation picture.^[4]

Through the above discussions on the DA reaction, we have shown that PIOs are usually localised orbitals with multi-centred feature still being preserved, which give rise to the good correspondence between PIOs and common chemical concepts. We have also demonstrated the ability for PIO to distinguish one scenario of DA reaction from the other, so that when it is applied to an unknown reaction, PIO analysis can offer great assistance for us to thoroughly understand and

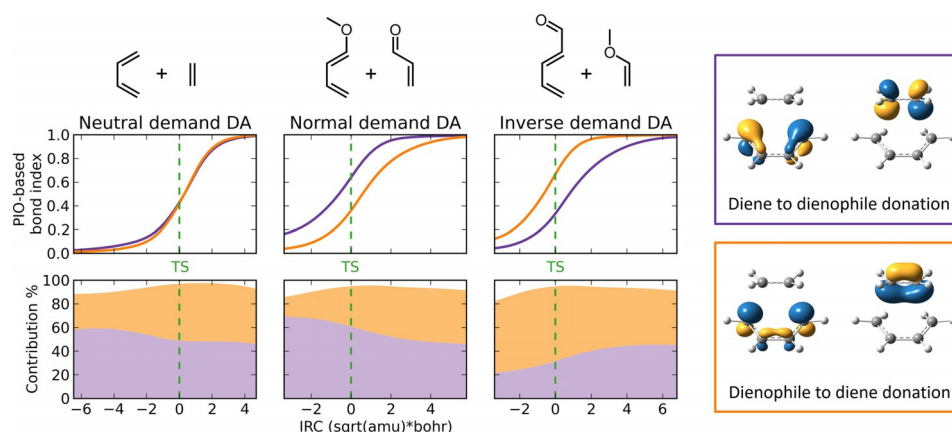


Figure 8. The evolution of PBI and contribution of top two PIO pairs against intrinsic reaction coordinate (IRC) in three DA reactions with different electron demands. The purple and orange curves correspond to the two PIO pairs shown on the right. Only representative PIOs from the simplest neutral DA reaction are shown here to label the plotted curves. The term “1st PIO pair” is not used here because it merely depends on the relative magnitude of each PBI at each point and may change over the course of reaction. Besides, three videos can be found in Supporting Information showing how the PIOs evolve with IRC for each system. Isovalue: 0.10.

properly classify the reaction, and finally find the key factor to reduce the reaction barrier if it is the rate-determining step of a complicated reaction.

Group 14 cluster compounds

Compared to ordinary organic compounds, bonding models for inorganic cluster compounds are often much more difficult to establish, because electrons in these compounds are highly delocalised. In the last section, we have shown that PIO analysis can identify the interacting functional groups and quantify their interaction magnitude. We are now going to demonstrate the power of PIO analysis through several much more challenging examples.

Our previous study on the cluster compound $[\text{Pd}_2\text{E}_{18}]^{4-}$ ($\text{E} = \text{Ge}, \text{Sn}$)^[29,30] revealed that two $[\text{Pd@E}_9]^{2-}$ moieties are not held together by conventional chemical bonds.^[31] Instead, their attraction results from a mutual delocalisation between their occupied MOs (OMOs) and unoccupied MOs (UMOs); in some sense similar to the scenario we just encountered in DA reactions. Such a conclusion was supported by Charge Decomposition Analysis (CDA), which projects the MOs of the whole molecule onto the MOs of two fragments.^[13] It has been found that each $[\text{Pd@E}_9]^{2-}$ fragment has a pair of degenerate LUMOs, which contributes the most (among all fragment UMOs) to the OMOs of the whole molecule. This indicates that the fragment LUMOs have been utilised to stabilise the OMOs of the other fragment, consequently leading to a net attraction between the two $[\text{Pd@E}_9]^{2-}$ fragments.

However, such a picture is built up from the tiny differences in the values given by CDA. Although the fragment LUMOs have slightly more contributions than other fragment UMOs from the CDA results, it is difficult to justify whether they are the only dominant interactions. The reason behind this is similar to what we have seen in Figure 6, that is, the “local” orbital interaction in our mind is actually contributed by a large number of delocalised orbitals. Thus the relative contributions of FMOs to each MO may not be sufficient to concisely describe the fragment interactions. In the light of these limitations of FMOs, we performed our PIO analysis on the compound $[\text{Pd}_2\text{Sn}_{18}]^{4-}$, to reinvestigate the orbital interactions between $[\text{Pd@Sn}_9]^{2-}$ moieties. The results are summarised in Figure 9.

Results show that the PIO analysis identifies not only two pairs of mutual delocalisations (the 3rd to 6th PIO pairs) of π -type symmetry, as also seen in our previous work, but also a pair of σ -type mutual delocalisation, with even slightly higher PBIs. Moreover, we can see that the accepting orbitals are quite localised on the three Sn atoms that are closest to the other fragment. In fact, they are just linear combinations of the tangential p-orbitals that are pointing towards the other fragment. On the other hand, the donating PIOs have more contribution from the middle layer of Sn atoms and also have more skeletal character.

One major advantage of the above analysis on fragment interactions is its good transferability. Transferability is of essential importance in chemistry, because it allows us to transfer

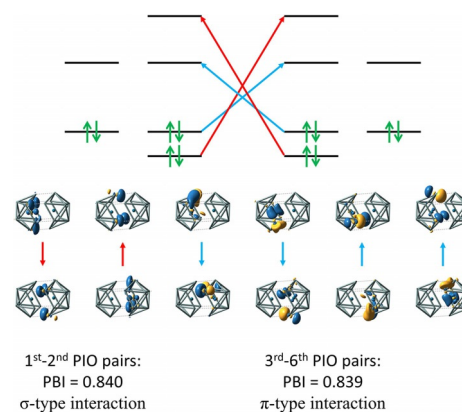


Figure 9. The top six PIOs of two $[\text{Pd@Sn}_9]$ fragments with respect to each other in $[\text{Pd}_2\text{Sn}_{18}]^{4-}$ cluster. Above is a schematic orbital diagram illustrating the mutual delocalisation between the two $[\text{Pd@Sn}_9]$ fragments. One pair of mutual delocalisation takes place between non-degenerate fragment orbitals which are labelled as σ -type and are described by the 1st and 2nd PIO pairs. The other two pairs of mutual delocalisation described by the 3rd-6th PIO pairs are labelled as π -type interactions.

our understanding of a chemical system into other similar ones, so that we can make predictions before performing experimental or computational studies. In particular, that is one of the reasons that FMO gains its wide use. For the same reason, chemists are motivated to use the aforementioned substituent-invariant description of DA reaction.

Here in this example, we have identified a group of “valence orbitals” of the $[\text{Pd@Sn}_9]^{2-}$ moiety, which could potentially be transferrable. These orbitals are not necessarily the HOMO/LUMOs of the moiety, but rather like “local HOMO/LUMOs” which are most willing to donate electrons to, or accept from, another moiety in similar geometries. To illustrate this, we take the compound $[\text{Ni}_2\text{Ge}_9\text{PPh}_3]^{2-}$ as an example,^[32] which has a $[\text{Ni@Ge}_9]^{2-}$ moiety which is isoelectronic to $[\text{Pd@Sn}_9]^{2-}$. We therefore view this compound as a coordination complex with $[\text{Ni@Ge}_9]^{2-}$ and PPh_3 as two ligands binding to a Ni centre. As we have identified the six “valence orbitals” (in the PIO sense) of $[\text{Pd@Sn}_9]^{2-}$, one of σ - and two of π -symmetry for both occupied and unoccupied orbitals, we would expect that the $[\text{Ni@Ge}_9]^{2-}$ moiety also uses these orbitals for its bonding with NiPPh_3 . The PIO analysis shows that this is indeed the case. From Figure 10, we can see that there are also six top PIO pairs in the $[\text{Ni}_2\text{Ge}_9\text{PPh}_3]^{2-}$ species, except that they are now grouped into two stronger σ - and four weaker π -type interactions. This is common for two-centred bonds because π -type orbitals are usually not as efficient as σ -type orbitals for bonding interactions. It is also interesting that both σ -type bonding and significant σ -type back-bonding are seen for the transition metal centre.

From the examination of the analogous role of $[\text{M@E}_9]$ fragment in the two different systems, we have shown in this section that PIO analysis can make it quite convenient for us to analyse fragment interactions and transfer them to similar cases, especially in complicated systems. This is benefited from our optimisation goal being interaction maximisation instead of direct electron localisation, so that a moderate electron lo-

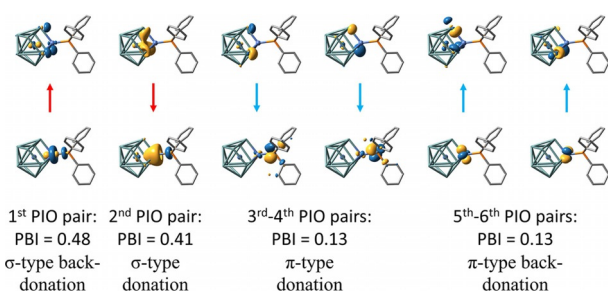


Figure 10. The top six PIO pairs of [Ni@Ge₉] and [NiPPh₃] fragments in the cluster compound [Ni₂Ge₉PPh₃]. The first two PIO pairs have larger PBIs and are σ-type interactions while the succeeding four π-type PIO pairs have smaller PBIs. Note that the PIOs of the [Ni@Ge₉] fragment are similar to those of [Pd@Sn₉] given in Figure 8.

calisation can be achieved without breaking the delocalised nature of orbital interaction.

Bifurcating reactions

Our success in analysing the DA reaction using PIO analysis inspired us to consider a more challenging class of reactions: the bifurcating reaction. A bifurcating reaction is a reaction in which a single transition state connects the reactant(s) and two different products (Figure 11 (b)) through a bifurcation point (more precisely, a valley-ridge inflection (VRI) point) on the potential energy surface (PES).^[33,34] Many examples of bifur-

cating reactions have been studied by Houk and his co-workers.^[33,35–39] However, it remains a difficult task to identify whether a reaction is a bifurcating reaction or not. Currently, one has to perform a scan on the PES around the transition state, to see if the transition state really leads to two different products (described as ambimodal), which, however, is quite expensive in terms of computational cost. In this section, we aim to use PIO analysis to quickly reveal the ambiguity of orbital interaction in the transition state to allow a quick identification of potentially bifurcating reactions.

We have chosen a recent example of a bifurcating reaction, in which a cycloaddition would take place in either a [6+4] or a [4+2] manner, but via the same transition state (Figure 11 (a)).^[36] Since there are multiple sites in the ambimodal transition state where bond formation and/or cleavage might take place, we are interested in how their orbitals are involved in this transition state.

Note that the selected reaction is an intra-molecular cycloaddition reaction, and there are no natural fragmentations that separate the reaction sites. Hence, we abandon a full fragmentation in which all the atoms are included. Instead, we adopt the fragmentation shown in Figure 11 (a). This fragmentation is adopted only because it is the minimum set that covers all the possible reaction sites and keeps each fragment connected. Other reasonable fragmentations also work and should give comparable results.

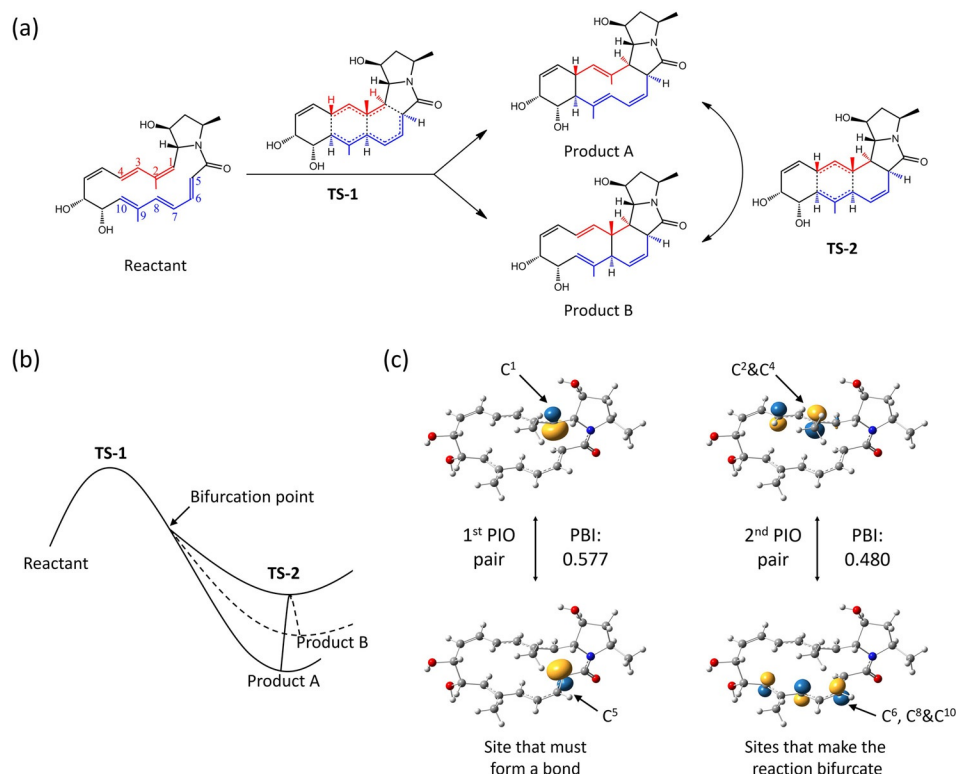


Figure 11. An example of bifurcating reaction and its PIO analysis. (a) The reaction equation of the selected example of bifurcating reaction. The atoms coloured in red and blue constitute fragments A and B, respectively, which would be used in the following PIO analysis. (b) A schematic plot of the potential energy surface of a bifurcating reaction. (c) The top two PIO pairs in TS-1. The total contribution of these two pairs are 94.8%, hence the rest of PIOs can be safely omitted in our context. The shapes of PIOs of TS-2 are similar to the orbitals shown here, and can be found in the Supporting Information if needed. Isovalue: 0.10.

The PIO analysis on **TS-1** shows that there are two dominant PIOs contributing 94.8% to the total interactions. However, the PIOs of fragment A resemble neither the HOMO/LUMO of hexatriene (for [6+4] cycloaddition) nor those of butadiene (for [4+2] cycloaddition), and the PIOs of fragment B resemble neither HOMO/LUMO of butadiene nor ethene. Interestingly, the 1st PIO of fragment A in **TS-1** is localised on a single atom, C¹, and the 1st PIO of fragment B is also localised on a single atom, C⁵. Given the fact that, no matter whether the system undergoes a [6+4] or [4+2] cycloaddition reaction, a bond would be formed between C¹ and C⁵, it is easy to understand why the interaction between C¹ and C⁵ is much stronger than other reaction sites as indicated by the first PIO pair.

The second PIO pair contributes almost equally, compared to the first PIO pair, to the total interactions between the two fragments. However, unlike the first PIO pair, the second pair of PIOs spread out on multiple sites in both fragments. It is easy to see that these sites are indeed the potential reaction sites and they have almost equal contributions, so that we cannot tell which site is more likely to form a bond. Such a situation remains in **TS-2**, at which point, strengthening the interaction of one site would weaken the interaction to the others, resulting in one of the two possible products (Supplementary Information Figure S2).

A side note is that, in this particular example, any full fragmentation would cut two σ -bonds and give rise to more PIOs with strong interactions, as the reaction sites locate in a cycle. We demonstrated this example here with a partial fragmentation to show that a full fragmentation is not necessary for analysing certain orbital interactions. A full fragmentation is, however, generally recommended if possible as it leads to the mathematically cleanest representation (as proved in Methods) and the availability of PIMOs.

To summarise, we show the PIO method can serve as a detector for bifurcating reactions, since it provides more information on the detailed orbital interaction. We believe a deeper understanding of electronic structure will certainly help us gain more chemical insights into these reactions.

Conclusions

In this paper, we have presented how our newly developed PIO analysis could be applied to analyse electronic structures, and aid our understanding on chemical structures and reactions. By determining the set of semi-localised orbitals (so-called PIOs) that best describe the interactions between two specified fragments in a chemical system, we develop a quantitative yet still intuitive picture of how chemical moieties bond to or affect each other. By forgoing a global scheme of localisation like NBO or AdNDP, we can better take into account the fragment of interest, and can adaptively analyse not only systems with distinctive Lewis structure, but also more delocalised systems like cluster compounds. The adoption of the PCA framework, together with the features of the density matrix from HF/DFT calculations, allows the mathematical elegance of PIOs that they only have a 1-to-1 interacting pattern.

We have demonstrated how PIO analysis could help us better understand various chemical phenomena. When applied to the analysis of electronic structures, PIOs allow us to identify less dominant interactions (like hyper-conjugation), which may be flooded out when we directly visualise MOs. When applied to analysis of reactions, PIOs allow us to identify orbital preferences, which will be helpful for rational design of substrates or ligands for reaction tuning.

It is also worth noting that PCA is a very popular tool in the field of machine learning,^[21] mostly for its distinctive ability of dimension reduction. While the top several PIOs can preserve a majority of interactions, the effect of truncating weaker interactions, that is, to set the interactions between tail PIO pairs to zero, will be minimised. This leads to the possibility that PIO method may be applied to local electron correlation methods for large systems and tight-binding models for periodic systems.

Experimental Section

Methods

Overview: In this section, we first give a concise description of the PIO method. We try to make the procedures easy to follow even for non-experts and non-programmers, because the algorithm itself is very short and simple, benefitting from the adoption of PCA framework. Necessary proofs and details, which would be rather technical, follow thereafter to establish mathematical foundations.

Construction and properties of PIOs: A first-order reduced density matrix (simply referred to as density matrix henceforth) is a concise representation of how electrons behave in a system. The density matrix can not only describe the population of an orbital (as a diagonal element) but also characterise the density correlation between two orbitals (as an off-diagonal element). The density matrix is very useful in analysing the electronic structure of a system, and has been utilised in the NBO analysis and the AdNDP methods. One of the most popular population analysis methods associated with NBO analysis, the Natural Population Analysis (NPA), constructs a set of Natural Atomic Orbitals (NAOs) associated with each atom, and determines the charge of an atom by subtracting the populations of all the NAOs belonging to this atom from its atomic number. The Wiberg Bond Index^[40] (WBI) calculates the square sum of the off-diagonal elements in a two-atom block in the NAO-based density matrix, as a measurement of the interaction magnitude between two atoms, and it turns out that WBI is more robust than the commonly used bond distance when one tries to quantify the extent to which two atoms interact with each other.

In the PIO analysis, we start with the NAO-based density matrix obtained from quantum chemistry calculations, denoted as D . When given a fragmentation of the system, as two groups of atoms, without loss of generality, D can be partitioned into blocks (by rearranging its rows and columns) [Eq. (1)]:

$$D = \begin{bmatrix} D_{AA} & D_{AB} & D_{AR} \\ D_{BA} & D_{BB} & D_{BR} \\ D_{RA} & D_{RB} & D_{RR} \end{bmatrix} \quad (1)$$

in which A and B represent the two fragments of interest and R collects the remaining atoms that are neither covered by A nor B.

In particular, the rows and columns of D_{AB} correspond to NAOs of atoms in fragment A and fragment B, respectively. The two fragments under study (A and B) should be non-empty and exclusive, while R can be empty if A and B cover all the atoms in the system. In order to obtain the PIOs of fragment A with respect to fragment B, one simply performs a Principal Component Analysis (PCA) on the off-diagonal block D_{AB} , viewing it as a collection of column vectors. PCA is a widely used technique in statistics,^[21] which aims to find the directions (unit vectors) that describe the largest variance of the input data (collection of vectors). Similarly, in the PIO analysis, we find the orbitals, as linear combinations of fragment NAOs, which describe the largest interactions (in terms of density correlation). Interested readers can see relevant text on PCA.^[21] A similar procedure performed on D_{BA} will yield PIOs of fragment B with respect to fragment A.

One of the most important properties of the PIO analysis is that the PIOs of fragment A and fragment B, with respect to each other, naturally form pairs. In other words, the 1st PIO of fragment A only interacts with the 1st PIO of fragment B, but not with any other PIOs of fragment B. Consequently, the PIO-based Bond Index (PBI) of a PIO pair is defined as the corresponding off-diagonal matrix element, that is, the matrix element whose row and column correspond to the PIOs of fragments A and B, respectively. The percentage contribution of a PIO pair is then defined as its PBI divided by the sum of PBIs of all the PIO pairs. Such a one-to-one interacting pattern conveniently enables us to analyse the fragment interaction in a pairwise manner.

Secondly, it is worth noting that a common and very important application of PCA is dimensionality reduction,^[21] which can also be inherited by the PIO analysis. While the top PIOs have the largest possible interactions, the tail PIOs have the least, so that it is possible to ignore them without significantly affecting the electronic structure of the whole system. That is why we only have to analyse several top PIOs in the presented examples. As we pointed out, it is natural to consider the interaction between two fragments in a hierarchical manner, that is to consider the strongest interactions first, followed by moderate and weaker interactions.

In addition, we can prove (given later in Technical Details) that the populations of a PIO pair are complementary to each other, that is, their populations add up to two. One should note that this is true only when the calculation is performed at the HF/DFT level and the fragmentation is full (i.e., R is empty). This property allows us to construct the so-called Principal Interacting Molecular Orbitals (PIMOs) by pairwise in-phase and out-of-phase linear combinations of PIO pairs. An in-phase combination of a PIO pair results in a PIMO with population exactly equal to two (one for each spin orbital), corresponding to the bonding orbital in the orbital interaction of this PIO pair, and an out-of-phase combination gives an empty PIMO corresponding to the anti-bonding orbital. As this property allows much cleaner results, we always try to find a full fragmentation in practice. For intramolecular reactions such as the previously discussed bifurcation reaction, one however often has to make a compromise: either choosing a full fragmentation which would give rise to several more dominant PIOs localised on the connecting atoms, or choosing an incomplete fragmentation that brings the interaction of interest to top, but loses a deterministic relationship between populations and PBIs.

We have also tested the influence of different basis sets on PIO analysis. It turns out that the results of PIO analysis are not sensitive to the choice of basis set (Supplementary Information Figure S21), as long as the basis set is reasonably large to guarantee the accuracy of quantum calculations and NAO construction. A similar test on functionals shows that most popular functionals

give comparable results while the Hartree–Fock method may have significant deviation in certain interactions (Supplementary Information Figure S22).

Last but not least, PCA is non-iterative and can be calculated very quickly. Consequently, a typical system with tens of atoms and moderate basis set only requires seconds to compute its PIOs.

Objective of PCA and relationship between PBI and WBI: In general, PCA works on a set of N sample vectors $\{X_k = (X_{k1}, X_{k2}, \dots, X_{kp})\}$, ($k = 1, 2, \dots, N$) in a p -dimensional space.^[21] PCA aims to determine a unit vector \hat{v}_1 [Eq. (2)] in the space that maximises the sum of projections of all the samples onto this vector:

$$\hat{v}_1 = \operatorname{argmax}_{\|\hat{v}_1\|^2=1} \left\{ \sum_k |X_k \cdot \hat{v}_1|^2 \right\} \quad (2)$$

This vector is named the first principal component (1st PC) of the sample vectors. Subsequent principal components are obtained through a similar process with additional orthogonality constraints. Although each principal component is defined to maximize each individual projection in a greedy manner, it turns out that the top k principal components also maximise the total projections of samples onto the subspace spanned by k vectors for any $1 \leq k \leq p$.^[21]

In PIO analysis, we treat each column in D_{AB} as a sample vector [Eq. (3)] and perform the PCA:

$$D_{AB} = (X_1 \quad X_2 \quad \dots \quad X_N) \quad (3)$$

Suppose the principal components obtained are [Eq. (4)]:

$$U = (\hat{v}_1 \quad \hat{v}_2 \quad \dots \quad \hat{v}_p)^T \quad (4)$$

The objective function that is maximised in PCA can be written as Equation (5):

$$\sum_k |X_k \cdot \hat{v}_1|^2 = \sum_k |(UD_{AB})_{jk}|^2 = \sum_k |(D'_{AB})_{jk}|^2 \quad (5)$$

where D'_{AB} is the new off-diagonal block in PIO representation. Thus the PCA process is actually determining a new representation of the matrix, such that the first column has the largest possible 2-norm, and the second column has the remaining largest one. Note that WBI is defined as Equation (6):

$$WBI_{AB} = \sum_{i \in A, j \in B} |D_{ij}|^2 \quad (6)$$

This reveals that our objective function is a generalisation of WBI. In this sense, we find the orbital in one fragment that has the largest generalised WBI with the orbitals of the other fragment. In the case that the two fragments under study are just two atoms, the summation of PBI of all the PIO pairs will reduce to the original WBI between these two atoms.

Proof of complementary populations of PIO pairs in HF/DFT calculations with full fragmentations: We now prove that, when the density matrix is obtained from HF/DFT calculations and fragments A and B cover all the atoms in the system, the populations of a PIO pair are complementary to each other. In such a case, the density matrix D satisfies that $D^2 = \lambda_D D$ because D only has one non-zero eigenvalue $\lambda_D = 2$ (assuming a restricted close-shell calculation). Then each eigenvector v of D_{AA} such that $D_{AA}v = \lambda v$ follows Equation (7).

$$D_{AB}D_{AB}^T\nu = \mathbb{P}DQ\mathbb{P}\nu = \mathbb{P}D(1-\mathbb{P})D\mathbb{P}\nu = \lambda_D\mathbb{P}D\mathbb{P}\nu - \mathbb{P}D\mathbb{P}\mathbb{P}D\mathbb{P}\nu = (\lambda_D\lambda - \lambda^2)\nu \quad (7)$$

where \mathbb{P} is the projection operator that projects the density matrix onto the space spanned by orbitals of fragment A only and $Q = 1 - \mathbb{P}$. Note that it is essential to the proof that $D^2 = \lambda_D D$. The above equation implies that ν is also an eigenvector of $D_{AB}D_{AB}^T$ with its eigenvalue being $(\lambda_D\lambda - \lambda^2)$. Therefore, as PIO representation diagonalises $D_{AB}D_{AB}^T$, it also diagonalises D_{AA} (up to degeneracy), and by symmetry D_{BB} is diagonalised as well.

Technical details: Suppose the off-diagonal block D_{AB} is of the dimensions $M \times N$, and its singular value decomposition (SVD) is $D_{AB} = USV^T$, where U and V are unitary matrices of dimensions $M \times M$ and $N \times N$, respectively, and S is a rectangular diagonal matrix of the dimensions $M \times N$. From the definition of PCA, the coefficient matrices of PIOs of fragments A and B in the NAO representation are eigenvectors of $D_{AB}D_{AB}^T$ and $D_{BA}D_{BA}^T$, respectively. It then follows that the coefficient matrices are just U and V , which can be easily proved from the relationship between SVD and PCA²¹. This means that the PIOs of fragments A and B can actually be obtained simultaneously by simply performing an SVD on D_{AB} . Furthermore, the rectangular diagonal matrix $S = U^T D_{AB} V$ is just the off-diagonal block of density matrix in the PIO representation, showing that PIOs of fragments A and B interact in a pairwise manner, which proves the one-to-one interacting pattern of PIOs. This results in a sparse representation of the interaction between fragments so that we can interpret the interaction pattern easily. It also follows that SVD automatically chooses the phases of PIOs such that each PIO pair always has a positive density correlation. The PIO-based bond indices (PBI) [Eq. (8)] are defined as the eigenvalues of $D_{AB}D_{AB}^T$ and $D_{BA}D_{BA}^T$, which are also related to the singular values of D_{AB} :

$$\lambda_{A,i} = \lambda_{B,i} = S_{ii}^2 \quad (8)$$

so the PBI of a PIO of fragment A is equal to the PBI of the corresponding PIO of fragment B. Thus in practice, PBI is used to describe the property of a PIO pair instead of a PIO of a single fragment.

A side note here is that fragments A and B may have different numbers of orbitals. It seems at the first glance that it is impossible for their PIOs to form pairs because of the conservation of number of orbitals. However, provided that the rank of the whole density matrix is $N/2$ (number of electron pairs, or N for unrestricted calculations), any fragment will not have more than $N/2$ PIOs. Because a finite basis set is adopted, a fragment with a smaller number of orbitals ($< N/2$) may have even fewer PIOs. In this case, the other fragment can only have the same number of non-trivial PIOs (trivial PIOs have a PBI of exactly zero).

This also ensures that PIO results are not sensitive to basis set selection, as long as it is reasonably large to guarantee the accuracy of quantum calculations and NAO construction. We also would like to mention that although different functionals can result in very different energies for one molecule, they usually give similar electron densities, and hence PIOs are also not sensitive to different functionals.

As PIOs are symmetry-preserving, there are cases that the system of interest has a high symmetry and the fragmentation retains some of the symmetry elements, which could lead to degenerate PIOs (in terms of PBI). In such a case, any linear combination of these degenerate PIOs gives exactly the same PBI, which can cause some arbitrariness. In practice, we always choose the representa-

tion that diagonalises the principal block D_{AA} , which will simultaneously diagonalise D_{BB} in HF/DFT calculations with full fragmentation from our previous proof.

Computational Details

All the quantum calculations are performed with the Gaussian09 package.^[41] All examples presented in main text and Supporting Information were optimised using the B3LYP functional^[42,43] combined with a 6-311++G(d,p) basis set^[44–47] for hydrogens and first-row elements, and the def2TZVP basis set (along with associated pseudopotentials if present)^[48] for all other elements except the following. Ethane was calculated under B3LYP/6-31G(d) level, and Diels–Alder reactions, as well as the umpolung reaction in Supporting Information, were calculated under M06-2X/6-31G(d).^[49,50] Two cluster compounds discussed in main text were calculated using PBE0 with a large def2TZVP basis set (along with associated pseudopotentials if present) for all atoms. Singlet point calculations were performed for the transition states of the bifurcating reaction with the geometries provided in the original work done by Houk's group using the same computational method (M06-2X/6-311++G(d,p)).^[36] NAOs are obtained using NBO6.0 software.^[11] The isovalues for drawing orbitals are specified in each Figure caption.

Code availability

Cartesian coordinates of all computed structures are available upon request. The code for PIO analysis is freely available at <https://github.com/jxzhgccc/PIO>.

Acknowledgements

This work was supported by the Research Grants Council of Hong Kong (N_HKUST603/15 and C5023-14G). The authors thank Prof. Hong Zhang for their fruitful discussions on metal-benzene and aromaticity, Dr. Zheng Wang for valuable discussions and suggestions on bifurcation reactions, and Miss Linlin Wu for her suggestions on Figure designs.

Conflict of interest

The authors declare no conflict of interest.

Keywords: bond theory • cluster compounds • electronic structure • orbital interaction • reaction mechanisms

- [1] R. B. Woodward, R. Hoffmann, *Angew. Chem. Int. Ed. Engl.* **1969**, *8*, 781–853; *Angew. Chem.* **1969**, *81*, 797–869.
- [2] R. Hoffmann, S. Alvarez, C. Mealli, F. Falceto, T. J. Cahill III, T. Zeng, G. Manca, *Chem. Rev.* **2016**, *116*, 8173–8192.
- [3] R. Hoffmann, *Acc. Chem. Res.* **1971**, *4*, 1–9.
- [4] K. Fukui, *Angew. Chem. Int. Ed. Engl.* **1982**, *21*, 801–809; *Angew. Chem.* **1982**, *94*, 852–861.
- [5] Applied Quantum Chemistry: Proceedings of the Nobel Laureate Symposium on Applied Quantum Chemistry in Honor of G. Herzberg, R. S. Mulliken, K. Fukui, W. Lipscomb, and R. Hoffman, Honolulu, HI, 16–21 December 1984 (Eds.: V. H. Smith Jr, H. F. Schaefer III, K. Morokuma).
- [6] "Theory of Orientation and Stereoselection": K. Fukui, *Reactivity and Structure: Concepts in Organic Chemistry*, Springer, Berlin, Heidelberg, **1975**.
- [7] K. Fukui, *Science* **1982**, *218*, 747.

- [8] "Localized Molecular Orbitals: A Bridge between Chemical Intuition and Molecular Quantum Mechanics": W. England, L. S. Salmon, K. Ruedenberg in *Molecular Orbital: Fortschritte der Chemischen Forschung*, Springer, Berlin, Heidelberg, **1971**, pp. 31–123.
- [9] F. K. Sheong, J.-X. Zhang, Z. Lin, *Coord. Chem. Rev.* **2017**, *345*, 42–53.
- [10] A. E. Reed, R. B. Weinstock, F. Weinhold, *J. Chem. Phys.* **1985**, *83*, 735.
- [11] E. D. Glendening, C. R. Landis, F. Weinhold, *J. Comput. Chem.* **2013**, *34*, 1429–1437.
- [12] A. E. Reed, F. Weinhold, *J. Chem. Phys.* **1985**, *83*, 1736.
- [13] S. Dapprich, G. Frenking, *J. Phys. Chem.* **1995**, *99*, 9352–9362.
- [14] D. Y. Zubarev, A. I. Boldyrev, *Phys. Chem. Chem. Phys.* **2008**, *10*, 5207–5217.
- [15] R. F. W. Bader, *Atoms in Molecules: A Quantum Theory; International Series of Monographs on Chemistry*, Oxford University Press, Oxford, **1994**.
- [16] J. Pipek, P. G. Mezey, *J. Chem. Phys.* **1989**, *90*, 4916–4926.
- [17] G. Knizia, *J. Chem. Theory Comput.* **2013**, *9*, 4834–4843.
- [18] D. Y. Zubarev, A. I. Boldyrev, *J. Phys. Chem. A* **2009**, *113*, 866–868.
- [19] A. P. Sergeeva, D. Y. Zubarev, H.-J. Zhai, A. I. Boldyrev, L.-S. Wang, *J. Am. Chem. Soc.* **2008**, *130*, 7244–7246.
- [20] B. B. Averkiev, D. Y. Zubarev, L.-M. Wang, W. Huang, L.-S. Wang, A. I. Boldyrev, *J. Am. Chem. Soc.* **2008**, *130*, 9248–9250.
- [21] I. T. Jolliffe, *Principal Component Analysis*, Springer, New York, **2002**.
- [22] V. Pophristic, L. Goodman, *Nature* **2001**, *411*, 565.
- [23] F. Weinhold, *Angew. Chem.* **2003**, *115*, 4320–4326.
- [24] G. E. Doublerly, A. M. Ricks, B. W. Ticknor, P. V. R. Schleyer, M. A. Duncan, *J. Am. Chem. Soc.* **2007**, *129*, 13782–13783.
- [25] S. Sieber, P. Buzek, P. V. R. Schleyer, W. Koch, J. W. D. M. Carneiro, *J. Am. Chem. Soc.* **1993**, *115*, 259–270.
- [26] F. A. Cotton, N. F. Curtis, C. B. Harris, B. F. G. Johnson, S. J. Lippard, J. T. Mague, W. R. Robinson, J. S. Wood, *Science* **1964**, *145*, 1305–1307.
- [27] F. A. Cotton, C. B. Harris, *Inorg. Chem.* **1965**, *4*, 330–333.
- [28] D. L. Boger, *Chem. Rev.* **1986**, *86*, 781–793.
- [29] Z.-M. Sun, H. Xiao, J. Li, L.-S. Wang, *J. Am. Chem. Soc.* **2007**, *129*, 9560–9561.
- [30] J. M. Goicoechea, S. C. Sevov, *J. Am. Chem. Soc.* **2005**, *127*, 7676–7677.
- [31] F. K. Sheong, W.-J. Chen, J.-X. Zhang, Y. Li, Z. Lin, *Dalton Trans.* **2017**, *46*, 2214–2219.
- [32] E. N. Esenturk, J. Fetting, B. Eichhorn, *Polyhedron* **2006**, *25*, 521–529.
- [33] D. H. Ess, S. E. Wheeler, R. G. Iafe, L. Xu, N. Celebi-Oelcuem, K. N. Houk, *Angew. Chem. Int. Ed.* **2008**, *47*, 7592–7601; *Angew. Chem.* **2008**, *120*, 7704–7713.
- [34] J. Rehbein, B. K. Carpenter, *Phys. Chem. Chem. Phys.* **2011**, *13*, 20906–20922.
- [35] N. Çelebi-Ölçüm, D. H. Ess, V. Aviyente, K. Houk, *J. Am. Chem. Soc.* **2007**, *129*, 4528–4529.
- [36] P. Yu, A. Patel, K. N. Houk, *J. Am. Chem. Soc.* **2015**, *137*, 13518–13523.
- [37] P. Yu, Z. Yang, Y. Liang, X. Hong, Y. Li, K. N. Houk, *J. Am. Chem. Soc.* **2016**, *138*, 8247–8252.
- [38] A. Patel, Z. Chen, Z. Yang, O. Gutierrez, H.-W. Liu, K. N. Houk, D. A. Singleton, *J. Am. Chem. Soc.* **2016**, *138*, 3631–3634.
- [39] P. Yu, T. Q. Chen, Z. Yang, C. Q. He, A. Patel, Y.-H. Lam, C.-Y. Liu, K. N. Houk, *J. Am. Chem. Soc.* **2017**, *139*, 8251–8258.
- [40] K. B. Wiberg, *Tetrahedron* **1968**, *24*, 1083–1096.
- [41] Gaussian 09, Revision D.01, M. J. Frisch, G. W. Trucks, H. B. Schlegel, G. E. Scuseria, M. A. Robb, J. R. Cheeseman, G. Scalmani, V. Barone, G. A. Petersson, H. Nakatsuji, X. Li, M. Caricato, A. Marenich, J. Bloino, B. G. Janesko, R. Gomperts, B. Mennucci, H. P. Hratchian, J. V. Ortiz, A. F. Izmaylov, J. L. Sonnenberg, D. Williams-Young, F. Ding, F. Lipparini, F. Egidi, J. Goings, B. Peng, A. Petrone, T. Henderson, D. Ranasinghe, V. G. Zakrzewski, J. Gao, N. Rega, G. Zheng, W. Liang, M. Hada, M. Ehara, K. Toyota, R. Fukuda, J. Hasegawa, M. Ishida, T. Nakajima, Y. Honda, O. Kitao, H. Nakai, T. Vreven, K. Throssell, J. A. Montgomery, Jr., J. E. Peralta, F. Ogliaro, M. Bearpark, J. J. Heyd, E. Brothers, K. N. Kudin, V. N. Staroverov, T. Keith, R. Kobayashi, J. Normand, K. Raghavachari, A. Rendell, J. C. Burant, S. S. Iyengar, J. Tomasi, M. Cossi, J. M. Millam, M. Klene, C. Adamo, R. Cammi, J. W. Ochterski, R. L. Martin, K. Morokuma, O. Farkas, J. B. Foresman, D. J. Fox, Gaussian, Inc., Wallingford CT, 2016.
- [42] A. D. Becke, *J. Chem. Phys.* **1993**, *98*, 5648–5652.
- [43] C. Lee, W. Yang, R. G. Parr, *Phys. Rev. B* **1988**, *37*, 785.
- [44] W. J. Hehre, R. Ditchfield, J. A. Pople, *J. Chem. Phys.* **1972**, *56*, 2257–2261.
- [45] P. C. Hariharan, J. A. Pople, *Theor. Chim. Acta.* **1973**, *28*, 213–222.
- [46] I. Deperasinska, J. A. Beswick, A. Tramer, *J. Chem. Phys.* **1979**, *71*, 2477–2487.
- [47] R. Ditchfield, W. J. Hehre, J. A. Pople, *J. Chem. Phys.* **1971**, *54*, 724–728.
- [48] F. Weigend, R. Ahlrichs, *Phys. Chem. Chem. Phys.* **2005**, *7*, 3297–3305.
- [49] Y. Zhao, D. G. Truhlar, *Acc. Chem. Res.* **2008**, *41*, 157–167.
- [50] Y. Zhao, D. G. Truhlar, *Theor. Chem. Acc.* **2008**, *120*, 215–241.

Manuscript received: March 10, 2018

Accepted manuscript online: April 17, 2018

Version of record online: June 13, 2018